Identification of Epstein-Barr Virus in the Human Placenta and Its Pathologic Characteristics

Younghoon Kim,[1,2] Hye Sung Kim,[3]
Joong Shin Park,[3] Chong Jai Kim,[4]
and Woo Ho Kim[1]

[1]Department of Pathology, Seoul National University College of Medicine, Seoul, Korea; [2]Laboratory of Epigenetics, Cancer Research Institute, Seoul National University, Seoul, Korea; [3]Department of Obstetrics and Gynecology, Seoul National University College of Medicine, Seoul, Korea; [4]Department of Pathology, University of Ulsan College of Medicine, Asan Medical Center, Seoul, Korea

Epstein-Barr virus (EBV), a common pathogen in humans, is suspected as the cause of multiple pregnancy-related pathologies including depression, preeclampsia, and stillbirth. Moreover, transmission of EBV through the placenta has been reported. However, the focus of EBV infection within the placenta has remained unknown to date. In this study, we proved the expression of latent EBV genes in the endometrial glandular epithelial cells of the placenta and investigated the cytological characteristics of these cells. Sixty-eight placentas were obtained from pregnant women. Tissue microarray was constructed. EBV latent genes including EBV-encoding RNA-1 (*EBER1*), Epstein-Barr virus nuclear antigen 1 (*EBNA1*), late membrane antigen (*LMP1*), and *RPMS1* were detected with silver in situ hybridization and/or mRNA in situ hybridization. Nuclear features of EBV-positive cells in EBV-infected placenta were compared with those of EBV-negative cells via image analysis. Sixteen placentas (23.5%) showed positive expression of all 4 EBV latent genes; only the glandular epithelial cells of the decidua showed EBV gene expression. EBV infection status was not significantly correlated with maternal, fetal, or placental factors. The nuclei of EBV-positive cells were significantly larger, longer, and round-shaped than those of EBV-negative cells regardless of EBV-infection status of the placenta. For the first time, evidence of EBV gene expression has been shown in placental tissues. Furthermore, we have characterized its cytological features, allowing screening of EBV infection through microscopic examination.

Keywords: Human Herpesvirus 4; Image Cytometry; In Situ Hybridization; Virus Latency; Decidua Capsularis

INTRODUCTION

Epstein-Barr virus (EBV) is a ubiquitous virus among the herpesvirus family, and is one of the most common viruses found in human (1,2). It is known to have tropism for B lymphocytes and specific types of epithelial cells (3). The B lymphocytes of more than 95% of adults worldwide have latent EBV infection. Several human diseases are associated with primary EBV infection in B lymphocytes, which includes infectious mononucleosis, various malignant lymphomas, lymphoproliferative disorders, and systemic autoimmune diseases (4,5). However, EBV infection in epithelial cells has been limited to the oropharynx, EBV-positive nasopharyngeal and gastric carcinomas, and oral hairy leukoplakia in patients with immunodeficiency status (6). Apart from these entities, evidence of latent EBV infection has not been confirmed in the epithelial cells.

Identification and characteristics of the EBV infection in the placenta has been elusive. A few papers argued that the EBV infection is associated with various pathologic conditions during pregnancy, including depression, preeclampsia, and stillbirth (7-9). These findings are mostly thought to be associated with

EBV infection of the B lymphocytes; confirmed by polymerase chain reaction (PCR) or serological tests with blood samples which do not involve histopathological information. On the other hand, vertical transmission of EBV during pregnancy through the placenta has been detected but the focus of EBV within the intrauterine environment has been poorly understood (10).

In the present study, we examined the expression of EBV-encoding RNA-1 (*EBER1*), the gold standard for detecting latent EBV infection in tissues (11), as well as three other EBV latent genes including Epstein-Barr virus nuclear antigen-1 (*EBNA1*), late membrane antigen (*LMP1*), and *RPMS1* gene encoding BamH1-a rightward transcript, to corroborate latent EBV infection in the placenta. Through this semi-quantitative method, expression of latent EBV genes in the glandular epithelium of the endometrium was specifically identified within the placenta. To the best of our knowledge, this is the first study to report the expression of EBV genes in the epithelial cell of the placenta. Furthermore, our study elucidates how EBV infection modifies the morphology of the epithelial cells, which has rarely been reported to occur in glandular epithelial cells.

MATERIALS AND METHODS

Placental tissues

We analyzed formalin-fixed and paraffin-embedded (FFPE) placental tissues collected from 68 pregnant women who underwent delivery at Seoul National University Hospital, Seoul, Korea from 2005 to 2016. They were randomly selected to include various gestation age from 26 to 39 weeks. Clinicopathological data such as maternal age, gestational age, gravity, parity, height, pre-pregnancy weight and body mass index (BMI), weight and BMI at delivery, proteinuria, blood pressure, history of labor induction, placental weight, fetal death, fetal weight, fetal gender, and Apgar scores were obtained from the electronic medical records. Histopathologic examination was done to evaluate the acute and chronic inflammatory status of placenta. This retrospective study was performed using stored samples at the Department of Pathology repository. Non-neoplastic uterine endometrial samples from 60 non-pregnant patients were selected for comparison.

Tissue microarray (TMA) construction

After histologic examination, four different cores of 2.0 mm in diameter were selected from each placenta, including one from the tissues of decidua capsularis in the chorioamniotic membrane. A separate TMA block comprising endometrial tissues from 60 non-pregnant women were also constructed. Clinical information of those 60 patients is summarized in Supplementary Table 1.

EBER1 silver in situ hybridization (SISH)

Four μm-thick sections were cut from each TMA block. The sections were subsequently deparaffinzied, dehydrated, digested with proteinase K, and hybridized for two hours at 37°C with dinitrophenyl (DNP)-conjugated probe targeting *EBER1* (Roche, Basel, Switzerland). Hybridization products were detected using a series of a rabbit anti-DNP antibody, a goat anti-rabbit secondary antibody conjugated with horseradish peroxidase (HRP), and chromogens. Metallic silver ions were visualized as black dots when silver ions were reduced by HRP, hydroquinone, and hydrogen peroxide. The staining results of TMA cores were confirmed with full sections of placenta tissues in a few EBV-positive cases.

mRNA in situ hybridization (ISH) by RNAscope

ISH was performed with RNAscope FFPE assay kit (Advanced Cell Diagnostics, Inc., Hayward, CA, USA) according to the manufacturer's instruction. The probes of the genes for ISH includes four latent genes (*EBER1, EBNA1, LMP1*, and *RPMS1*) and two lytic genes (BamH1 Z fragment first leftward open reading frame [*BZLF1*] and BamH1 M fragment first rightward open reading frame [*BMRF1*]). In brief, 4-μm TMA sections were heated and digested for pretreatment. The sections were hybridized with probes that target *EBNA1, EBER1, LMP1, RPMS1, BZLF1*, or *BMRF1*. Each target probe contains a 25-base region complementary to the target RNA, a spacer sequence, and a 14-base tail sequence, called Z probe. A pair of target probes (ZZ probe), each possessing a different type of tail sequence, hybridize contiguously to a target region (50 bases). The two tail sequences together form a 28-base hybridization site for the preamplifier, which contains 20 binding sites for the amplifier, that, in turn, contains 20 binding sites for the label probe. Thereafter, a HRP-based signal amplification system was applied to target probe before color development with 3,3′-diaminobenzidine. The *EBNA1* probe consists of 18 pairs of ZZ probes spanning 56–1,006 bp region of the *EBNA1* gene. The *EBER1* probe consisted of two pairs of ZZ probes spanning 39–120 bp region of the *EBER1* gene. The *RPMS1* probe consisted of 20 pairs of ZZ probes spanning 16,917–18,206 bp region. The *BZLF1* probe consisted of 14 pairs of ZZ probes spanning 2–701 bp region. The *BMRF1* probe consisted of 20 pairs of ZZ probes spanning 2–1,204 bp region. Positive staining was defined as brown dots or clusters within the boundary of the cellular membrane including nucleus and cytoplasm. The housekeeping gene ubiquitin C served as a positive control for intact mRNA. The *DapB* gene, encoding *Bacillus subtilis* dihydrodipicolinate reductase, was used as a negative control.

Immunohistochemistry

TMA sections in 4 μm-thickness were deparaffinized in xylene and were rehydrated with gradually decreasing concentrations of alcohol. The sections were immunostained using a Ventana Benchmark XT automated immunostainer with OptiView amplification kit (Roche) according to the manufacturer's instructions. The primary antibodies used were anti-E-cadherin (1:100; Leica Biosystems, New Castel, UK), anti-cytokeratin (1:300; DAKO, Glostrup, Denmark), and anti-CD31 (1:50; DAKO). E-cadherin and cytokeratin were stained at the cell membrane and cytoplasm of epithelial cells. CD31 staining was positive at the cell membrane of endothelial cells.

Morphometric assessment of EBV-infected cells

Each TMA slides were scanned by the Aperio image analysis system (Leica Biosystems). To compare the nuclear properties of EBV-infected and EBV-uninfected cells in endometrial glandular epithelial cells, CellProfiler image analysis software (http://www.cellprofiler.org) was used (12). Fifty-one nuclei from EBV-positive cells, 128 nuclei from EBV-negative cells of EBV-infected placental tissues, and 95 nuclei from EBV-negative cells of EBV-uninfected placental tissues were analyzed. Briefly, endometrial glandular epithelial cells that were stained with hematoxylin for nuclear staining were captured at 400×. Each snapshot underwent an identical pipeline that determined the nu-

clear properties of glandular cells. The variables that were saved as pixels were converted into micrometer units.

Statistical analysis

All statistical analysis was performed using SPSS (version 22.0; IBM Corp., Armonk, NY, USA). The correlation between EBV-positivity and clinicopathological variables were determined using the χ^2 test, Fisher's exact test, or Student's t-test, as appropriate. Results were considered statistically significant when P values were less than 0.05.

Ethics statement

The study design was approved by the Institutional Review Board of Seoul National University Hospital (reference No. H-1704-151-848) under the condition that the informed consent of individual patients was waived.

RESULTS

EBER1 SISH and RNAscope in placental tissues

The presence of latent EBV infection has never been reported in the placenta. *EBER1* probe manufactured from Roche (for-
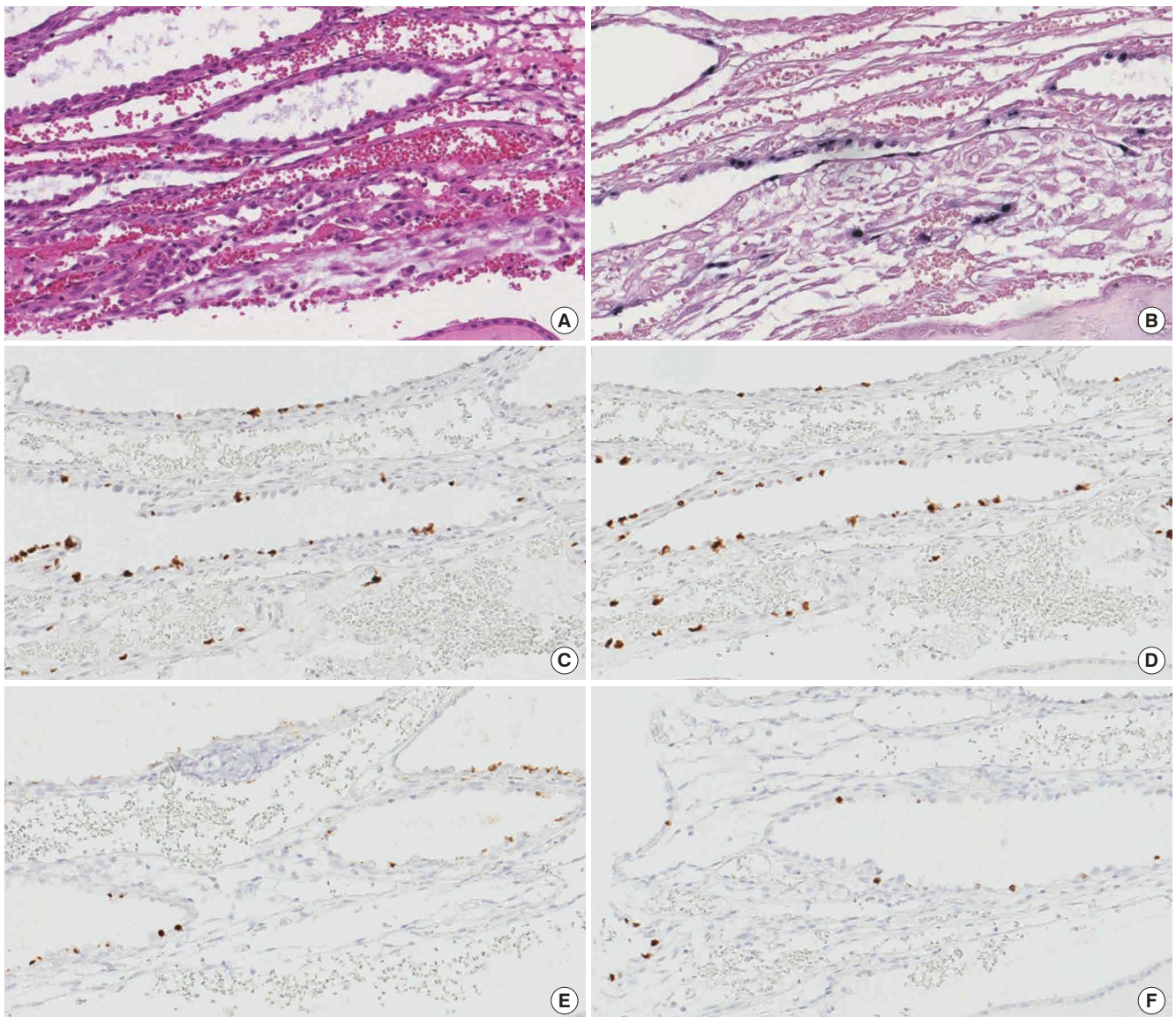
Fig. 1. Expression of various viral genes in an EBV-positive case. Hematoxylin-eosin staining (**A**). Positive staining is represented by black color in SISH of *EBER1* gene by Ventana (**B**). ISH staining by RNAscopy of four EBV latent genes, including *EBER1* (**C**), *EBNA1* (**D**), *LMP1* (**E**), and *RPMS1* (**F**) was positive demonstrating the brown color at the nucleus.
EBV = Epstein-Barr virus, SISH = silver in situ hybridization, *EBER1* = EBV-encoding RNA-1, ISH = in situ hybridization, *EBNA1* = Epstein-Barr virus nuclear antigen-1, *LMP1* = late membrane antigen.

merly Ventana) was used to perform SISH on placental TMA. We found EBV-positive cell in 16 out of 68 placentas examined (23.5%). *EBER1*-positive cells were only found in the decidua of the chorioamniotic membranes, and these were cuboidal glandular epithelial cells with round to oval nuclei arranged in a single layer which surrounded the dilated lumina containing se-

cretory materials (Fig. 1A and 1B). We verified our finding by performing mRNA ISH using RNAscope to detect *EBER1*, *EBNA1*, *LMP1*, and *RPMS1* genes, markers of latent gene expression in EBV (Fig. 1C to 1F). The results of all four latent genes demonstrated that positivity matched exactly at the same cells, although the intensity of the staining was slightly different. In contrast,
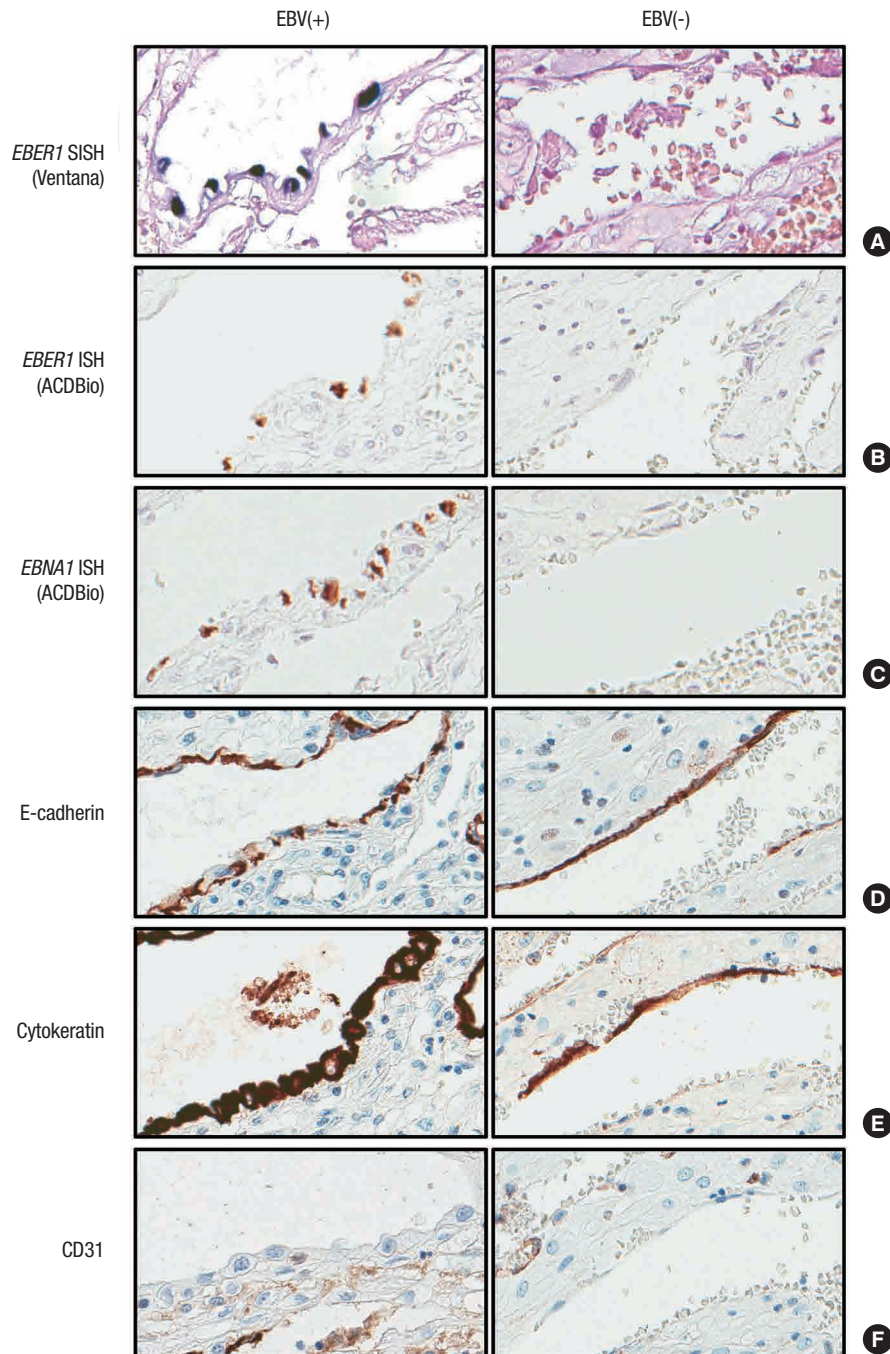
Fig. 2. Comparison of endometrial glands in the decidua of EBV-infected (left) and EBV-uninfected (right) chorioamniotic membranes. *EBER1* SISH (**A**), *EBER1* mRNA ISH (**B**), and *EBNA1* mRNA ISH (**C**) were positive only in EBV-infected cases. Immunohistochemical staining of epithelial cells was positive for E-cadherin (**D**) and cytokeratin (**E**) and was negative for CD31 (**F**) regardless of EBV infection.
EBV = Epstein-Barr virus, *EBER1* = EBV-encoding RNA-1, SISH = silver in situ hybridization, ISH = in situ hybridization, *EBNA1* = Epstein-Barr virus nuclear antigen-1.

lytic genes including *BZLF1* and *BMRF1* were evaluated as negative in any of the cells in the placenta since the stained cells were positive for E-cadherin and cytokeratin, but were negative for CD31, the stained cells were further confirmed as glandular epithelial cell of the decidua (Fig. 2). None of the cells derived from fetal cells, including various trophoblasts, stromal cells, and amniotic epithelial cells are positively stained on any of EBV-derived probes. Maternal cells such as decidual stromal cells, endothelial cells, and cells derived from maternal blood were not stained with EBV-derived probes, either (Table 1). Sixty non-pregnant uterine samples that included various stages of endometrium did not display any evidence of EBV gene expression.

Correlation between EBV-positive cells and clinicopathological variables

The association between EBV infection status and clinicopathological features were investigated (Table 2). Maternal and gestational ages were not correlated with EBV infection status. Although maternal history of fullterm delivery, preterm delivery, spontaneous abortion, and artificial abortion was more frequent in EBV-uninfected patients than in EBV-infected patients, it did not meet statistical significance. Other maternal conditions such as maternal height, pre- and post-pregnancy BMIs, proteinuria, systolic and diastolic blood pressures, blood glucose level, and history of labor induction were not associated with EBV infection. EBV infection also did not show any significant association with fetal conditions, which included fetal death, fetal weight, fetal gender, and Apgar scores evaluated at 1 minute and 5 minutes after birth. EBV infection was not significantly associated with placental factors including placental weight, and acute or chronic placental inflammations, either.

Morphometry of EBV-positive cells

Viral members of the herpesvirus family affect cell morphology in infected epithelial cells, but rarely in glandular epithelial cells (13,14). In this study, distinct cytological features such as nuclear inclusion, less condense chromatin contour, increased nu-

Table 1. Positive rate of EBV in placental tissues

| Cell types	Percentage (positive/placentas)
Fetal cells	
Syncytiotrophoblasts/cytotrophoblasts/indeterminate trophoblasts	0 (0/68)
Hofbauer cells/fibroblast/endothelial cells	0 (0/68)
Amniotic epithelial cells	0 (0/68)
Maternal cells	
Decidual endometrial stromal cells	0 (0/68)
Decidual endometrial epithelial cells	23.5 (16/68)
Endothelial cells/leucocytes	0 (0/68)

EBV = Epstein-Barr virus.

Table 2. Comparison of clinicopathological features between the patients with EBV(+) and EBV(–) placentas

| Clinical features	EBV status		*P* value
	Negative (n = 52)	Positive (n = 16)	
Maternal age (range), yr	33.06 ± 3.70 (26–43)	33.06 ± 4.17 (27–40)	0.998
Gestational age at delivery, day	242.21 ± 26.67	241.56 ± 26.85	0.933
Fullterm delivery history			0.231
0	33	7	
1–2	18	9	
Preterm delivery history			1.000
0	47	15	
1	4	1	
Spontaneous abortion history			0.427
0	43	12	
1–3	6	3	
Artificial abortion history			0.669
0	46	14	
1–2	2	2	
Maternal height, cm	161.56 ± 5.52	161.64 ± 5.47	0.962
Pre-pregnancy BMI, kg/m^2	21.37 ± 4.04	23.14 ± 4.62	0.196
Post-pregnancy BMI, kg/m^2	25.51 ± 4.71	27.95 ± 5.29	0.113
Proteinuria			0.428
0	46	14	
1+–4+	1	1	
Systolic BP, mmHg	116.12 ± 14.68	123.19 ± 11.29	0.081
Diastolic BP, mmHg	74.46 ± 13.29	75.63 ± 10.83	0.751
Blood glucose, mg/dL	94.05 ± 21.54	83.08 ± 11.06	0.085
Labor induction history			1.000
No	44	14	
Yes	7	2	
Fetal death			1.000
Alive	49	16	
Dead	2	0	
Fetal weight, kg	2.30 ± 0.92	2.40 ± 0.92	0.693
Fetal gender			0.764
Male	43	12	
Female	21	4	
Apgar score 1 min			0.665
> 7	26	7	
≤ 7	23	8	
Apgar score 5 min			0.770
> 7	15	4	
≤ 7	34	11	
Placental weight, g	576.92 ± 233.11	500.00 ± 160.26	0.233
Acute chorioamnionitis			1.000
Absent	31	9	
Present	21	7	
Acute funisitis			1.000
Absent	47	15	
Present	5	1	
Acute inflammation			0.567
Absent	27	7	
Present	25	9	
Chronic villitis			0.342
Absent	48	13	
Present	4	3	
Chronic chorioamnionitis			1.000
Absent	37	12	
Present	15	4	
Chronic deciduitis			0.689
Absent	45	13	
Present	7	3	
Chronic inflammation			0.769
Absent	33	9	
Present	19	7	

Data are shown as mean ± standard deviation.
EBV = Epstein-Barr virus, BMI = body mass index, BP = blood pressure.

EBV(+)   EBV(-)
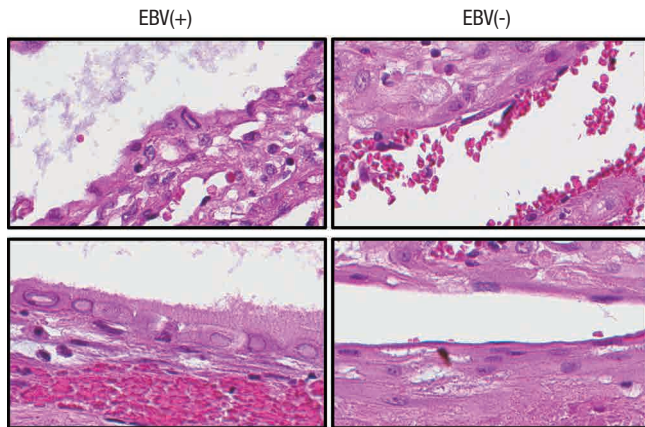
Fig. 3. Cytological difference between EBV-positive (left) and EBV-negative glandular epithelial cells. Epithelial cells positive for EBV latent gene expression show drastic cellular changes including nuclear inclusion, less condense chromatin contour, increased nucleus and cytoplasm in volume, and perinuclear clearing of cytoplasm. EBV = Epstein-Barr virus.

EBV(+) cells (EBV-infected placenta)

EBV(-) cells (EBV-infected placenta)

EBV(-) cells (EBV-uninfected placenta)

Fig. 4. Example of difference in nuclear morphology based on EBV-positivity of individual cells. These nuclei were included in the analysis for objective comparison (Supplementary Table 2).
EBV = Epstein-Barr virus.

cleus and cytoplasm in volume, and perinuclear clearing of cytoplasm were observed in EBV-positive cells (Figs. 3 and 4). To objectify the impact of EBV gene expression on cellular phenotype, nuclear features of EBV-infected and EBV-uninfected placental tissues were investigated through image analysis (Supplementary Table 2). Nuclei from EBV-infected samples were further categorized according to EBV-positivity status determined by *EBER1* ISH. EBV-positive cells had significantly larger nuclear area and increased nuclear perimeter than EBV-negative cells derived from EBV-infected placentas ($P < 0.001$) and the EBV-uninfected placentas ($P < 0.001$). The nuclei of EBV-positive cells also had a significantly longer minor axis length ($P < 0.001$), and a significantly greater maximum Feret diameter, minimum Feret diameter, maximum radius, mean radius, and median radius than those of EBV-negative cells ($P = 0.028$, $P < 0.001$, $P < 0.001$, $P < 0.001$, $P < 0.001$, and $P < 0.001$, respectively for cells derived from EBV-infected cases and $P = 0.009$, $P < 0.001$, $P < 0.001$, $P < 0.001$, $P < 0.001$, and $P < 0.001$, respectively for cells derived from EBV-uninfected cases). However, the difference in major axis length of the nuclei between EBV-positive and EBV-negative cells were only marginal within EBV-infected samples ($P = 0.058$) but were significant when compared with EBV-uninfected samples ($P = 0.019$). The nuclei of EBV-positive cells were significantly more circular in shape compared with those of EBV-negative cells from EBV-infected and EBV-uninfected samples as deduced from smaller compactness ($P = 0.001$ and $P < 0.001$, respectively), smaller eccentricity ($P < 0.001$ and $P < 0.001$, respectively), larger extent ($P < 0.001$ and $P < 0.001$, respectively), and larger form factor ($P < 0.001$ and $P = 0.009$, respectively). Moreover, nuclear features of EBV-negative cells from EBV-infected samples and EBV-uninfected samples showed overlapping results ($P > 0.05$).
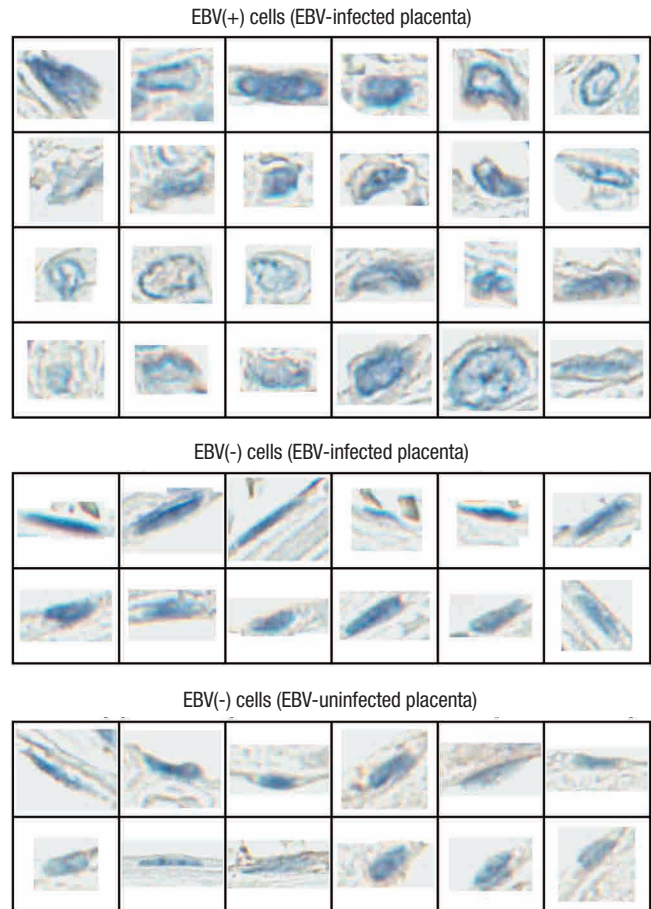
DISCUSSION

EBV expression in epithelial cells has been known to be limited to specific histologic and anatomical location, namely the oropharynx, a few types of carcinomas, and immunocompromised status, such as oral hairy leukoplakia (6). Outside these examples, evidence of latent EBV infection has not been clearly confirmed, even with the *EBER1* SISH as the gold standard to detect EBV infection in tissues, especially in non-pathological conditions. For example, Martínez-López et al. (15) displayed *EBER1* expression in gastric epithelial cells of the gastritis cases. However, positive cells are most likely B lymphocytes since the density of *EBER1*-positive cells were much higher than cells positive for cytokeratin. *EBER1* ISH staining in the gingival epithelium suggested by Vincent-Bugnas et al. (16) lacks the follow-up results observed in similar experiments. In addition, the study does not discuss about the nuclear change overtly observed in EBV-positive cells. Therefore, to the best of our knowledge, this is the first study to authenticate latent EBV infection of glandular epithelial cells outside the oropharynx without neoplastic

condition or immunocompromised disorder being present.

In the present study, positive staining for *EBER1* was limited to glandular epithelial cells in the decidua with no other type of cells demonstrating positivity. Expression of *EBNA1, LMP1,* and *RPMS1* was confirmed alongside *EBER1* expression, further confirming latent EBV infection. EBV-positive cells had a distinct morphology that could be distinguished not only from EBV-negative cells of EBV-uninfected cases but also EBV-negative cells of EBV-infected placenta. The nuclei of EBV-positive cells were larger, longer, rounder, had a less condensed chromatin, and had more abundant cytoplasm compared with those of EBV-negative cells. Interestingly, acute or chronic placental inflammations were not associated with EBV gene expression. Moreover, amniotic epithelial cells that has been used to transfer EBV under experimental conditions in the past (17) did not express EBV latent genes even in EBV-infected placentas. CD21 is a cellular receptor for the EBV entry into human B cells. However, cellular receptor for epithelial cell is not well recognized. We examined the expression of CD21 in the placenta, and confirmed that all the fetal and maternal cells in the placenta including EBV-positive cells did not express CD21 (data not shown).

Regarding the limitation of our study, we could not identify the underlying mechanism of EBV infection in the decidua while endometrium in non-pregnant patients did not show any trace of EBV infection. We hypothesize that the microenvironment of the placenta, which is specialized in fetomaternal tolerance, plays a vital role. The placenta has immunosuppressing functions that leads to immune tolerance during pregnancy. Programmed cell death-ligand 1 (PD-L1), which regulates the immune checkpoint pathway, is expressed in placental trophoblasts and amniotic epithelial cells to secrete immunosuppressive factors that reduce lymphocyte proliferation. If immune tolerance is not maintained, deleterious consequences of inflammation or fetal rejection may occur (18,19). This sophisticated microenvironment, which is often referred to as an immune privilege site (20), may explain why EBV is accepted in the placenta. In addition, local blockage of PD-L1 in the epithelial cell resulted in increased viral clearance of influenza virus in the lung, furthers implying that co-expression of PD-L1 and EBV latent genes in the placenta might not be a coincidence (21). Therefore, while the placental and the chorioamniotic membranes act as physical and biological barriers to resist against viral infection (22), its function in fetomaternal tolerance may act as a gateway which is susceptible to EBV infection in the maternal decidua, specifically the glandular epithelial cells. Future studies should investigate the adverse effects of the EBV infection within the decidua. Another limitation of this study is that we examined only four cores from each placenta with TMA methodology. Consequently, the positive rate of EBV infection in this paper (23.5%) might have a chance to be underestimated.

In conclusion, we have identified EBV genes as a novel viral agent that could be detected in the glandular epithelium of the decidua. Our study also determined that EBV infection could be screened using microscopic examination, as such infection is associated with specific nuclear changes in the endometrial epithelial cells of the placenta.

DISCLOSURE

The authors have no potential conflicts of interest to disclose.

AUTHOR CONTRIBUTION

Conceptualization: Park JS, Kim WH. Data curation: Kim Y, Kim HS, Kim WH. Formal analysis: Kim Y, Kim WH. Methodology: Kim Y, Kim CJ, Kim WH. Software: Kim Y, Kim HS.

ORCID

Younghoon Kim https://orcid.org/0000-0003-4656-0188
Hye Sung Kim https://orcid.org/0000-0002-3522-2864
Joong Shin Park https://orcid.org/0000-0002-5246-0477
Chong Jai Kim https://orcid.org/0000-0002-2844-9446
Woo Ho Kim https://orcid.org/0000-0003-0557-1016

REFERENCES

1. Chang MS, Lee HS, Kim CW, Kim YI, Kim WH. Clinicopathologic characteristics of Epstein-Barr virus-incorporated gastric cancers in Korea. *Pathol Res Pract* 2001; 197: 395-400.

2. Fleisher G, Henle W, Henle G, Lennette ET, Biggar RJ. Primary infection with Epstein-Barr virus in infants in the United States: clinical and serologic observations. *J Infect Dis* 1979; 139: 553-8.

3. Borza CM, Hutt-Fletcher LM. Alternate replication in B cells and epithelial cells switches tropism of Epstein-Barr virus. *Nat Med* 2002; 8: 594-9.

4. Okano M, Gross TG. Acute or chronic life-threatening diseases associated with Epstein-Barr virus infection. *Am J Med Sci* 2012; 343: 483-9.

5. Draborg AH, Duus K, Houen G. Epstein-Barr virus in systemic autoimmune diseases. *Clin Dev Immunol* 2013; 2013: 535738.

6. Tugizov S, Herrera R, Veluppillai P, Greenspan J, Greenspan D, Palefsky JM. Epstein-Barr virus (EBV)-infected monocytes facilitate dissemination of EBV within the oral mucosal epithelium. *J Virol* 2007; 81: 5484-96.

7. Zhu P, Chen YJ, Hao JH, Ge JF, Huang K, Tao RX, Jiang XM, Tao FB. Maternal depressive symptoms related to Epstein-Barr virus reactivation in late pregnancy. *Sci Rep* 2013; 3: 3096.

8. Elliott SE, Parchim NF, Kellems RE, Xia Y, Soffici AR, Daugherty PS. A preeclampsia-associated Epstein-Barr virus antibody cross-reacts with placental GPR50. *Clin Immunol* 2016; 168: 64-71.

9. Tomai XH. Stillbirth following severe symmetric fetal growth restriction due to reactivation of Epstein-Barr virus infection in pregnancy. *J Obstet Gynaecol Res* 2011; 37: 1877-82.

10. Meyohas MC, Maréchal V, Desire N, Bouillie J, Frottier J, Nicolas JC. Study of mother-to-child Epstein-Barr virus transmission by means of nested PCRs. *J Virol* 1996; 70: 6816-9.

11. Braz-Silva PH, de Rezende NP, Ortega KL, de Macedo Santos RT, de Magalhães MH. Detection of the Epstein-Barr virus (EBV) by in situ hybridization as definitive diagnosis of hairy leukoplakia. *Head Neck Pathol* 2008; 2: 19-24.

12. Carpenter AE, Jones TR, Lamprecht MR, Clarke C, Kang IH, Friman O, Guertin DA, Chang JH, Lindquist RA, Moffat J, et al. CellProfiler: image analysis software for identifying and quantifying cell phenotypes. *Genome Biol* 2006; 7: R100.

13. Iwasaka T, Kidera Y, Tsugitomi H, Sugimori H. The cellular changes in primary and recurrent infection with herpes simplex virus type 2 in an in vitro model. *Acta Cytol* 1987; 31: 935-40.

14. Juric-Sekhar G, Upton MP, Swanson PE, Westerhoff M. Cytomegalovirus (CMV) in gastrointestinal mucosal biopsies: should a pathologist perform CMV immunohistochemistry if the clinician requests it? *Hum Pathol* 2017; 60: 11-5.

15. Martínez-López JL, Torres J, Camorlinga-Ponce M, Mantilla A, Leal YA, Fuentes-Pananá EM. Evidence of Epstein-Barr virus association with gastric cancer and non-atrophic gastritis. *Viruses* 2014; 6: 301-18.

16. Vincent-Bugnas S, Vitale S, Mouline CC, Khaali W, Charbit Y, Mahler P, Prêcheur I, Hofman P, Maryanski JL, Doglio A. EBV infection is common in gingival epithelial cells of the periodontium and worsens during chronic periodontitis. *PLoS One* 2013; 8: e80336.

17. Al-Moslih MI, White RJ, Dubes GR. Use of a transfection method to demonstrate a monolayer cell transforming agent from the EB3 line of Burkitt's lymphoma cells. *J Gen Virol* 1976; 31: 331-45.

18. Guleria I, Khosroshahi A, Ansari MJ, Habicht A, Azuma M, Yagita H, Noelle RJ, Coyle A, Mellor AL, Khoury SJ, et al. A critical role for the programmed death ligand 1 in fetomaternal tolerance. *J Exp Med* 2005; 202: 231-7.

19. Prasad S, Hu S, Sheng WS, Chauhan P, Singh A, Lokensgard JR. The PD-1: PD-L1 pathway promotes development of brain-resident memory T cells following acute viral encephalitis. *J Neuroinflammation* 2017; 14: 82.

20. Okazaki T, Honjo T. The PD-1-PD-L pathway in immunological tolerance. *Trends Immunol* 2006; 27: 195-201.

21. McNally B, Ye F, Willette M, Flaño E. Local blockade of epithelial PDL-1 in the airways enhances T cell function and viral clearance during influenza virus infection. *J Virol* 2013; 87: 12916-24.

22. Delorme-Axford E, Sadovsky Y, Coyne CB. The placenta as a barrier to viral infections. *Annu Rev Virol* 2014; 1: 133-46.

Supplementary Table 1. Clinical information of the 60 non-pregnant patients whose endometrial tissues were used as control for EBV staining

Parameters	No. of patients
Sex	
Female	60
Male	0
Age, yr	
Mean ± SD	38.83 ± 4.22
Range	25–45
Phase	
Proliferative	27
Secretory	33
Underlying disease	
Benign	46
Malignant	14

EBV = Epstein-Barr virus, SD = standard deviation.

Supplementary Table 2. Nuclear features of EBV-positive cells compared with those of EBV-negative cells from EBV-infected or uninfected placental tissues

Nuclear features	1. EBV(+) (n = 51)	2. EBV(–) (n = 128) (EBV-infected)	3. EBV(–) (n = 95) (EBV-uninfected)	P value (1 vs. 2)	P value (1 vs. 3)
Area, μm²	59.78 ± 28.1	31.55 ± 12.33	30.38 ± 12.84	< 0.001	< 0.001
Compactness	1.44 ± 0.48	2.02 ± 1.69	1.88 ± 0.81	0.001	< 0.001
Eccentricity	0.81 ± 0.14	0.93 ± 0.05	0.91 ± 0.08	< 0.001	< 0.001
Extent	0.67 ± 0.11	0.56 ± 0.14	0.58 ± 0.15	< 0.001	< 0.001
Form factor	0.61 ± 0.14	0.52 ± 0.12	0.55 ± 0.14	< 0.001	0.009
Major axis length, μm	12.84 ± 5.44	11.29 ± 2.95	10.98 ± 3.96	0.058	0.019
Minor axis length, μm	6.25 ± 1.49	3.74 ± 0.91	3.76 ± 1.00	< 0.001	< 0.001
Maximum Feret diameter, μm	12.64 ± 5.11	10.93 ± 2.87	10.65 ± 3.85	0.028	0.009
Minimum Feret diameter, μm	6.31 ± 1.53	3.74 ± 0.92	3.70 ± 1.03	< 0.001	< 0.001
Maximum radius, μm	2.92 ± 0.68	1.82 ± 0.43	1.81 ± 0.47	< 0.001	< 0.001
Mean radius, μm	1.17 ± 0.23	0.80 ± 0.16	0.80 ± 0.17	< 0.001	< 0.001
Median radius, μm	1.07 ± 0.22	0.73 ± 0.15	0.73 ± 0.15	< 0.001	< 0.001
Perimeter, μm	35.24 ± 11.55	27.56 ± 6.54	26.87 ± 8.06	< 0.001	< 0.001

Data are shown as mean ± standard deviation.
EBV = Epstein-Barr virus.